Title: Hydraulic flux-responsive hormone redistribution determines root branching

Authors: Poonam Mehra[1]*, Bipin K. Pandey[1], Dalia Melebari[1], Jason Banda[1], Nicola Leftley[1], Valentin Couveur[2], James Rowe[3], Moran Anfang[4], Hugues De Gernier[5,6], Emily Morris[1†], Craig J. Sturrock[1], Sacha J. Mooney[1], Ranjan Swarup[1], Christine Faulkner[7], Tom Beeckman[5,6], Rishikesh P. Bhalerao[8], Eilon Shani[4], Alexander M. Jones[3], Ian C. Dodd[9], Robert E. Sharp[10], Ari Sadanandom[11], Xavier Draye[2], Malcolm J. Bennett[1]*

Affiliations:

[1]*Plant and Crop Sciences, School of Biosciences, University of Nottingham; LE12 5RD, UK.*

[2]*Earth and Life Institute, Université catholique de Louvain; 1348 Louvain-la-Neuve, Belgium.*

[3]*Sainsbury Laboratory, University of Cambridge; 47 Bateman Street, Cambridge CB2 1LR, UK.*

[4]*School of Plant Sciences and Food Security, Tel Aviv University; Tel Aviv, Israel.*

[5]*Department of Plant Biotechnology and Bioinformatics, Ghent University; Ghent 9052, Belgium.*

[6]*Center for Plant Systems Biology, VIB-UGent; Ghent 9052, Belgium*

[7]*Crop Genetics, John Innes Centre, Norwich Research Park; Norwich, UK.*

[8]*Umeå Plant Science Centre, Department of Forest Genetics and Plant Physiology, Swedish University of Agricultural Sciences; SE-901 87 Umeå, Sweden.*

[9]*Lancaster Environment Centre, Lancaster University; Lancaster, UK.*

[10]*Division of Plant Science and Technology, University of Missouri; Columbia, MO, United States.*

[11]*Department of Biosciences, University of Durham; Durham, DH1 3LE, UK.*

†*Present address: Oxford University Innovation; Oxford, UK*

*Corresponding author Email(s):

p.mehra@nottingham.ac.uk (P.M), malcolm.bennett@nottingham.ac.uk (M.J.B)

Abstract: Plant roots exhibit plasticity in their branching patterns to forage efficiently for heterogeneously distributed resources such as soil water. The xerobranching response represses lateral root formation when roots lose contact with water. Here we show that xerobranching is regulated by radial movement of phloem-derived hormone abscisic acid (ABA), which disrupts intercellular communication between inner and outer cell layers via plasmodesmata. Closure of these inter-cellular pores disrupts the inward movement of the hormone signal auxin, blocking lateral root branching. Once root tips regain contact with moisture, the ABA response rapidly attenuates. Our study reveals how roots adapt their branching pattern to heterogeneous soil water conditions by linking changes in hydraulic flux with dynamic hormone redistribution.

One-Sentence Summary: Transient water stress suppresses root branching by linking changes in hydraulic flux with dynamic hormone redistribution.

Main Text:

Root branching determines foraging capacity of crop plants (*1, 2*). Roots have evolved plasticity in their branching patterns to maximise access to soil water resources, which are often distributed heterogeneously (*3*, *4*). Root branching is affected both by extreme weather (such as drought or flooding) (*5*, *6*) and by transient or local spatial differences in soil moisture (*7, 8*). Negative effects of water scarcity on modern agriculture will be exacerbated as climate change impacts hydrological cycles and soil water resources (*9*, *10*). Increased resilience in the face of climate change will require better insight into how plant roots sense and adapt to fluctuating water availability.

Dissecting root water sensing using xerobranching

Xerobranching (*7*) provides an experimental model to study root adaptive responses to transient water stress. A xerobranching response is triggered when growing root tips temporarily lose contact with moist soil (e.g. in an air-gap), causing branching to temporarily cease until roots re-enter moist soil (Fig. 1A). To discover the mechanistic basis of xerobranching, an agar-based xerobranching bioassay was developed (fig. S1) which phenocopies the original X-ray Computed Tomography (CT) soil-based bioassay (Fig. 1A) in experiments with *Arabidopsis* and tomato seedlings. As levels of the abiotic stress signal abscisic acid (ABA) increase in root tips during transient water stress (*7*), we tested whether tomato ABA biosynthesis mutants (*flacca* and *notabilis*) (*11*, *12*) are disrupted in xerobranching response. Both soil- and agar-based bioassays revealed that, unlike wild-type (WT) controls, primary roots of both *flacca* and *notabilis* continue to branch when growing across an air-gap (Fig. 1, A to D and fig. S2). Similarly, the ABA deficient maize mutant *vp14* (*13*) disrupted xerobranching both in paper-based and soil-based bioassays (figs. S3 and S4). Hence, ABA is a widely conserved regulator that represses lateral root development during a xerobranching response in these monocot and eudicot plant models.

In which tissue(s) does ABA originate from to trigger a xerobranching response? ABA biosynthesis genes like *ABA2* are expressed in phloem-related root vascular tissues (*14*). *Arabidopsis aba2-1* mutant roots exhibit a xerobranching defect, which can be rescued by expressing WT *ABA2* using the phloem companion cell-expressed *SUC2* promoter (Fig. 1, E to G and fig. S5A). A *SUC2:YFP-ABA2* translation fusion confirmed that the ABA2 protein can act in a phloem companion cell-autonomous manner (fig. S5B). Phloem provides water for growing roots in the temporary absence of an external supply (*15*). Hydraulic modelling (*16*, *17*) predicts radial water fluxes within root tissues change direction from predominately inwards to outwards following a xerobranching stimulus (Fig. 1H). Simulations reveal that an inwards water flux dominates under normal externally hydrated conditions, and phloem-derived water is limited to close to companion cells (Fig. 1H). However, following a xerobranching stimulus (when the external water source is temporarily lost), root tip tissues rely on an outwards flux of phloem-derived water to maintain growth, requiring ~8 hours for outer root tissues to receive phloem water (Fig. 1H). Phloem-derived ABA is likely to travel with this outwards flow of water during a xerobranching response.

ABA moves outwards following a xerobranching stimulus

To visualise *whether*, *when* and *where* ABA movement occurs following a xerobranching stimulus, we utilised a sensitive FRET-based hormone biosensor (*18*), nlsABACUS2 which displays increased fluorescence emission ratio upon ABA binding (fig. S6). Seedlings expressing a nuclear localised nlsABACUS2 biosensor revealed dynamic changes in ABA distribution and levels during our agar-based xerobranching bioassay (Fig. 1, I to K and figs. S7 and S8). Spatially, nlsABACUS2 accumulates in epidermal cells in the basal meristem and

elongation zones (Fig. 1J). Quantifying temporal emission ratio changes revealed that ABA levels initially increase in root epidermal tissues >12 hours after a xerobranching stimulus. Considering the sensitivity of biosensor, these results are also consistent with our hydraulic simulations that predict outward flux of phloem-derived water after ~8 hours of xerobranching stimulus (Fig. 1H). Once root tips re-connect with the agar (recovery phase), ABA levels fall rapidly in epidermal cells (Fig. 1, J and K and fig. S8).

To directly visualise *whether* ABA moves radially outwards ("piggy-backing" the re-direction of water flux) following a xerobranching stimulus, we generated cross-sectional images of nlsABACUS2 root tip tissues (Fig. 2) from three key zones. These zones included meristem and early elongation zone tissues (zone 1), mid to late elongation and early differentiation zone tissues (zone 2) and fully differentiated root tissues (zone 3). Radial images of these three zones (taken at different time points during the xerobranching response) revealed contrasting patterns of ABA redistribution. For example, an increase in ABA levels can initially be detected in inner root tissues that is later seen in outer tissues in zone 2 (compare nlsABACUS2 signals in 3mm versus 4mm root tip sections for zone 2 in Fig. 2) consistent with ABA movement from inner to outer root tissues. In contrast, radial cross sections through nlsABACUS2 zone 1 root tissues revealed an increase in ABA in outer (but not inner) tissues, suggesting this signal originates from phloem unloading in zone 2 and then undergoes redistribution via symplastic continuity. ABA accumulated much less in outer root tissues of zone 3 versus zones 1 and 2 following a xerobranching stimulus (Fig. 2). The results are consistent with the phloem unloading patterns of solutes described earlier (*19*) suggesting that zone 2 overlaps with the protophloem unloading zone where solutes are transferred laterally via symplastic continuity. In contrast, zone 3 is active in solute translocation through phloem but inactive in phloem unloading (*19*). Another parallel study also reports similar expression patterns of nlsABACUS, when exogenously applied ABA unloads through phloem (*18*). The pattern of elevated ABA in outer root tissues of zones 1 and 2 also coincide with the root tip region where new lateral root primordia initiate (termed the basal meristem or oscillatory zone) (*20*, *21*). Elevated levels of ABA in zones 1 and 2 rapidly reduce once root tip tissues contact a new moisture source during the recovery phase (Fig. 2). Endogenous ABA levels in cotyledons of nlsABACUS2 plants did not change following a xerobranching stimulus, suggesting that ABA accumulation is locally confined to root tips exposed to air-gaps (figs. S7 to S9). Hence, during a xerobranching response ABA accumulates in the root zone associated with the earliest stage of lateral root development.

To test the function of the observed changes in ABA following a xerobranching stimulus, we examined the impact of mutations in key components of the ABA signalling machinery for this adaptive response. ABA insensitive mutants disrupting ABA receptors (*pyr/pyl*) and ABA-activated SnRK2 kinases (*snrk2.2/2.3*, *snrk2.2/2.3/2.6*) exhibited lateral root branching in our xerobranching bioassay (Fig. 3A and figs. S10 and S11), whilst ABA hypersensitive *pp2c* mutants failed to produce lateral roots in the air-gap (fig. S12). Detailed analysis with *snrk* triple/septuple/nonuple mutants as well as *snrk2.2* complementation lines revealed that *SnRK2.2* is required for xerobranching (Fig. 3D and fig. S11). Roots of a *snrk* nonuple mutant (lacking nine out of ten members of the SnRK2 family except SnRK2.2) behaved like WT in our xerobranching bioassay (fig. S11). Furthermore, a GFP-tagged SnRK2.2 reporter *pSnRK2.2: SnRK2.2-GFP* revealed that a xerobranching stimulus induced the fusion protein in the basal root meristem (Fig. 3B and C and fig. S13), which overlaps with the site of largest emission ratio changes of ABA biosensor nlsABACUS2 (Fig. 1J). Hence, SnRK2.2 regulates ABA (and in turn the xerobranching) response in *Arabidopsis* root tissues.

ABA regulates xerobranching by closing plasmodesmata

Genetic and biosensor-based studies revealed that ABA moves from its inner root (phloem) source to outer root tissues during a xerobranching response (Fig. 1, E to H, J; Fig. 2 and Fig. 3B). However, it remains unclear which root tissue(s) ABA targets to repress lateral root development during a xerobranching response. To determine this, we attempted to rescue the xerobranching defect of the ABA response mutant *snrk2.2/2.3* by expressing the WT *SnRK2.2* sequence under a series of root tissue/zone specific promoters (Fig. 3, E to J). Expressing *SnRK2.2* in either root epidermal, cortical, endodermal, or basal meristem (but not lateral root cap) tissues rescued the *snrk2.2/2.3* xerobranching defect (Fig. 3, E to J). This result led us to ask, is there a common target important for xerobranching that the ABA signalling pathway regulates in each of these outer root tissues? ABA modulates hydraulic conductivity by inducing aquaporin expression to affect water movement out of the vasculature (*22*). To investigate possible roles of aquaporins in ABA-dependent repression of branching in air-gaps, we analysed *pip* (Plasma membrane Intrinsic Proteins) quadruple mutant in our xerobranching bioassay system. However, analysis of *pip* mutant disrupting the most highly expressed *PIP* genes in roots did not show any significant difference compared to the WT control (fig. S14).

ABA has been reported to trigger reversible closure of intercellular pores termed plasmodesmata (PD) (*23*). Does ABA regulate the xerobranching response by gating plasmodesmata between root tissues? To address this, the symplastic fluorescent tracer carboxyfluorescein (CF; derived from CFDA, carboxy-fluorescein diacetate) was used to monitor whether plasmodesmata were open or shut in root tissues during a xerobranching response. Within plant cells, non-fluorescent CFDA is cleaved by cellular esterases to release membrane-impermeable fluorescent CF that travels exclusively through the plasmodesmata. Following CFDA application to cotyledons, we observed decreased protophloem unloading in *Arabidopsis* WT root tips exposed to a xerobranching stimulus (fig. S15). Delayed unloading was also observed in root tips of a *pSUC2:GFP* line that expresses free GFP in phloem companion cells (fig. S16). Collectively, both lines of evidence reveal that root tips experience decreased plasmodesmata permeability following a xerobranching stimulus.

To assess the role of ABA in root PD gating during xerobranching, CFDA was locally applied to root tips. WT roots exhibited reduced intercellular fluxes of the tracer, indicating closed plasmodesmata following a xerobranching stimulus (Fig. 4, A and B). In contrast, CFDA treatment of root tips of the ABA response mutant *snrk2.2/2.3* revealed that plasmodesmata remained open following a xerobranching stimulus (fig. S17). Plasmodesmata aperture is regulated by modifying the size of a callose 'ring' encircling each end of the inter-cellular pore. The callose stain aniline blue revealed higher callose deposition in basal meristem cells of WT roots compared to *snrk2.2/2.3* following a xerobranching stimulus (fig. S18). Taken together, the evidence indicates that ABA regulates gating of plasmodesmata in key root tissues during a xerobranching response.

To determine the function of plasmodesmata gating during a xerobranching response, *Arabidopsis* mutants no longer able to gate their plasmodesmata were characterised (figs. S19 and S20). Plasmodesmata aperture is regulated through the action of enzymes including a family of Callose Synthases (CS) and associated regulatory proteins like plasmodesmata-located proteins (PDLPs) (*24*). Mutating individual members of the *Arabidopsis* CS gene family resulted in nine of these lines exhibiting a xerobranching defect, including *CALS7* which is primarily associated with phloem sieve pores (*25*) (fig. S19), as did mutating both *PDLP2* and *PDLP3* genes (fig. S20). Hence, blocking the ability to close plasmodesmata disrupts a root's ability to activate a xerobranching response.

How does ABA trigger plasmodesmata closure following a xerobranching stimulus? Transgenic lines expressing GFP reporters fused to either PDLP2 or PDLP3 proteins under their native promoters were upregulated in response to a xerobranching stimulus (Fig. 4, C and

D and figs. S21, S22 and S23). In the case of PDLP3, its mRNA and *PDLP3:PDLP3-GFP* reporter were upregulated in root tip and specifically basal meristem cells during a xerobranching response, exhibiting a punctate pattern in apical, basal and side walls, consistent with its plasmodesmata regulatory function (Fig. 4, C and D and figs. S21 and S23). Treating roots of *PDLP3:PDLP3-GFP* with low levels of ABA (50 nM) phenocopied a xerobranching stimulus (fig. S24), in agreement with the presence of several ABA-responsive elements (ABRE) in its promoter sequence (Table S1). We also noted that many other *PDLP* and *Callose Synthase* genes contained ABREs in their promoter sequences (Table S1 and S2). Comparing spatio-temporal response curves of nlsABACUS2 and PDLP3-GFP (during xerobranching and subsequent recovery) reveals that ABA accumulation precedes PDLP3 induction (Fig. 1K and fig. S23). To test the functional importance of ABA regulated PDLP upregulation during xerobranching, we characterised the ABA-insensitive mutant *abi1-1*. The dominant negative *abi1-1* allele disrupts ABA-dependent plasmodesmata closure and maintains high frequencies of open plasmodesmata (*26*). Unlike WT, *abi1-1* roots exhibit branching in air-gaps (fig. S25). However, ectopic expression of *PDLP1* (using *35S* rather than its native promoter) rescued the xerobranching defect of *abi1-1* (fig. S25). Hence, ABA triggers plasmodesmata closure following a xerobranching stimulus by upregulating expression of *PDLP*s. Additionally, GAL4-mediated transactivation of *abi1-1* in root ground tissues (cortex and endodermis) led to maximal disruption of xerobranching response as compared to induction of *abi1-1* in single root cell layers (fig. S26). Hence, ABA mediated PD closure in root ground tissues is essential for a xerobranching response.

Plasmodesmata closure blocks inwards auxin movement

How does ABA-mediated plasmodesmata gating disrupt lateral root branching? Our reporter studies reveal that closing plasmodesmata during a xerobranching response blocks the inwards (symplastic) movement of another plant hormone signal, auxin, which is required to initiate lateral root branching. Exposing roots of the *DR5:VENUS* auxin reporter line to a xerobranching stimulus results in an elevated auxin response in epidermal cells within the root basal meristem zone (Fig. 4, E and F). The altered *DR5:VENUS* reporter pattern is consistent with xerobranching-induced PD closure in basal meristem epidermal cells transiently blocking the radially-inward symplastic movement of auxin (Fig. 4, E and F and fig. S27). The auxin reporter DII-VENUS also revealed higher auxin abundance in root tips during exposure to a xerobranching stimulus (figs. S27 and S28). The effect of a xerobranching stimulus on *DR5:VENUS* and DII-VENUS can be mimicked by exogenous application of ABA to roots (Fig. 4, G and H and fig. S29). ABA-mediated plasmodesmata gating during a xerobranching response blocks radial inward auxin movement and lateral root induction. Consistent with this model, switching off ABA signalling in the *abi1-1* mutant (which ensured that plasmodesmata remained constitutively open) blocked any change in DII-VENUS auxin response following a xerobranching stimulus (fig. S30). Suppression of lateral root initiation in roots exposed to a xerobranching stimulus was visualised using the *DR5:LUC* reporter, which normally demarks groups of lateral root stem cells in the basal meristem (or oscillation zone) that go on to form new branches in control roots, but were not detected in roots exposed to a xerobranching stimulus (fig. S31). Hence, the xerobranching response blocks radially-inward symplastic auxin movement that is required for lateral root induction.

Root auxin distribution was originally thought to be exclusively determined by the combined activities of AUX1/LAX, ABCB and PIN auxin influx and efflux carriers (*27*). To determine the impact of xerobranching on carrier-mediated auxin transport, reporter lines for key auxin influx (*pAUX1:AUX1-YFP*) or efflux (*pPIN2:PIN2-GFP*) carriers expressed in the root elongation zone were analysed (fig. S32). No spatial changes were detected in AUX1-YFP or PIN2-GFP expression in the outermost root tissues following a xerobranching stimulus,

consistent with the observed elevated auxin response (Fig. 4, E and F and fig. S27) being due to gating of hormone movement through plasmodesmata rather than via modulation of apoplastic auxin transport (fig. S32). Ectopic expression of either *AUX1* or *PIN2* in every elongation zone tissue to create a synthetic radial apoplastic auxin pathway, successfully bypassed the plasmodesmata-mediated restriction of symplastic auxin flow and led to lateral root branching in air-gaps (fig. S33).

Collectively, multiple lines of evidence establish a role for ABA-mediated plasmodesmata gating of radial symplastic auxin flow to regulate xerobranching. Roots appear to 'sense' water availability by co-mobilising water and hormones via plasmodesmata. If water, ABA and auxin moved through substrate specific carriers (i.e. aquaporins, ABCG and PINs), their co-mobilisation would be broken. Instead, because plasmodesmata are large inter-cellular pores that are non-selective, radial hydraulic fluxes co-mobilise hormones either inwards (like auxin) or outwards (like ABA) when water is available or not, respectively. Thus, auxin and ABA can be considered as "hydrosignals" when co-mobilised via plasmodesmata with water.

Our study has revealed that xerobranching is a widely conserved, ABA-dependent root adaptive response to localized loss of contact with soil water in eudicot and monocot species. We also report the molecular and cellular mechanisms enabling plant roots to block lateral root formation after experiencing a xerobranching stimulus (see schematic in Fig. 5). Under optimal moisture conditions, roots co-transport auxin and water inwards between root basal meristem tissues via plasmodesmata, providing a symplastic pathway to radially mobilise this key hormone signal with hydraulic fluxes from epidermal to pericycle cells, where auxin triggers lateral root initiation. However, when the external source of water is transiently unavailable, root tips rely on an internal (phloem) source of water to continue growing (*15*) and couple its outwards radial flow with movement of the hormone ABA. This key water stress signal reduces plasmodesmata aperture, disrupting radial movement of the branching signal auxin to lateral root 'stem cells' in the pericycle. Restoring an external water source (during the re-set/recovery phase) rapidly reduces ABA levels in the outermost root tissues (>3 hours), restoring open plasmodesmata and symplastic auxin transport. Once re-connected with an external water source, the abundance and distribution of these signals re-set in root tip tissues to pre-xerobranching stimulus levels. These dynamic regulatory events, coupling changes in hydraulic fluxes with hormone redistribution which we term hydrosignalling, enable plant roots to calibrate spatial root branching responses in heterogenous soil environments, which are the norm rather than the exception. Climate change is likely to exacerbate water scarcity *(9, 10)*, thus it is highly likely that water in soils will be even more heterogeneously distributed than at present. Insight into the molecular and cellular mechanisms through which roots acclimate under these conditions may improve the climate resilience of future crops.

References and Notes

1. B. Muller *et al*., *Trends Plant Sci*. **24**, 810-825 (2019).
2. J. P. Lynch, *Plant Physiol*. **156**, 1041-1049 (2011).
3. H. Motte, T. Beeckman, *J. Exp. Bot*. **70**, 785-793 (2019).
4. E. C. Morris *et al., Curr. Biol*. **27**, R919-930 (2017).
5. A. Zhan, H. Schneider, J. P. Lynch, *Plant Physiol.* **168**, 1603-1615 (2015).
6. R. Karlova, D. Boer, S. Hayes, C. Testerink, *Plant Physiol.* **187**, 1057-1070 (2021).
7. B. Orman-Ligeza *et al*., *Curr. Biol.* **28**, 3165-3173 (2018).
8. Y. Bao *et al*., *Proc. Natl. Acad. Sci. U.S.A.* **111**, 9319–9324 (2014).
9. D. B. Lobell, S. M. Gourdji, *Plant Physiol.* **160**, 1686-1697 (2012).
10. Y. Grusson, I. Wesström, E. Svedberg, A. Joel, *Agric. Water Manag.* **249**, 106766 (2021).

11. A. J. Thompson, E. T. Thorne, A. Burbidge, A. C. Jackson, R. E. Sharp, I. B. Taylor, *Plant Cell Environ*. **27**, 459-471 (2004).
12. I. B. Taylor, R.S. T. Linforth, R. J. Al-Naieb, W. R. Bowman, B. A. Marples, *Plant Cell Environ*. **11**, 739-745 (1988).
13. B. C. Tan, S. H. Schwartz, J. A. D. Zeevaart, D. R. McCarty, *Proc. Natl. Acad. Sci. U.S.A.* **94**, 12235-12240 (1997).
14. T. Kuromori, E. Sugimoto, K. Shinozaki, *Plant Physiol.* **164**, 1587-1592 (2014).
15. B. S. Wiegers, A. Y. Cheer, W.K. Silk, *Plant Physiol*. **150**, 2092-2103 (2009).
16. V. Couvreur, M. Faget, G. Lobet, M. Javaux, F. Chaumont, X. Draye, *Plant Physiol*. **178**, 1689-1703 (2018).
17. F. C. Pascut *et al*., *Nat. Commu.* **12**, 1-7 (2021).
18. J. Rowe *et al*., (*Under review*).
19. T. J. Ross-Elliott *et al*., *elife* **6**, p.e24125 (2017).
20. I. De Smet *et al*., *Development* **134**, 681-690 (2007).
21. M. A. Moreno-Risueno, J. M. Van Norman, A. Moreno, J. Zhang, S. E. Ahnert, P. N. Benfey, *Science* **329**, 1306-1311 (2010).
22. K. Prado *et al*., *Plant Cell* **25**, 1029-1039 (2013).
23. Y. Benitez-Alfonso, *Plant Cell Physiol.* **60**, 713-714 (2019).
24. C. L. Thomas, E. M. Bayer, C. Ritzenthaler, L. Fernandez-Calvino, A. J. Maule AJ, *PLoS Biol* **6**, e7 (2008).
25. B. Xie, X. Wang, M. Zhu, Z. Zhang, Z. Hong, *Plant J.* **65**, 1-14 (2011).
26. S. Tylewicz *et al*., *Science* **360**, 212-215 (2018).
27. J. Petrasek, J. Friml, *Development* **136**, 2675-2688 (2009).
28. D. Dietrich *et al.*, *Nat. Plants* **3**, 1-8 (2017).
29. G. Brunoud *et al*., *Nature* **482**, 103-106 (2012).
30. R. Bhosale *et al*., *Nat. Commun.* **9**, 1-9. (2018).
31. B. Péret *et al*., *Plant Cell* **24**, 2874-2885.
32. R. Swarup *et al*., *Plant Cell* **16**, 3069-3083 (2004).
33. M. C. Caillaud *et al*., *PLoS Pathog.* **10**, e1004496 (2014).
34. L. Kong *et al*., *Nat. Commun.* **6**, 1-3 (2015).
35. P. Ramachandran *et al*., *Curr. Biol.* **31**, 3153-3161 (2021).
36. S.K. Singh, C. Eland, J. Harholt, H.V. Scheller, A. Marchant, *Plant J.* **43**, 384-397 (2005).
37. G. Reyt *et al*., *Curr. Biol.* **30**, 4103-4111 (2020).
38. B. K. Pandey *et al*., *Science* **371**, 276-280 (2021).
39. P. Perrochet, D. Bérod, *Water Resour. Res.* **29**, 3291-3297 (1993).
40. M.P. Pound, A. P. French, D. M. Wells, M. J. Bennett, T. P. Pridmore, *Plant Cell* **24**, 1353-1361 (2012).
41. C. Andème-Onzighi, M. Sivaguru, J. Judy-March, T.I. Baskin, A. Driouich, *Planta* **215**, 949-958 (2002).
42. T. Zhu, W.J. Lucas, T.L. Rost, *Protoplasma* **203**, 35-47 (1998).
43. J. Pritchard, *J. Exp. Bot.* **47**, 1519-1524 (1996).
44. D. Hall, A.R. Evans, H.J. Newbury, J. Pritchard, *J. Exp. Bot.* **57**, 1201-1210 (2006).
45. X. Yang, G. Dong, K. Palaniappan, G. Mi, T.I. Baskin, *Plant Cell Environ.* **40**, 264-276 (2017).
46. R. Siligato *et al*., *Plant Physiol.* **170**, 627-641 (2016).
47. M. Karimi, B. D. Meyer, P. Hilson, *Trends Plant Sci.* **10**, 103-105 (2005).
48. F.A. Engelen, J. W. Molthoff, A. J. Conner, J. P. Nap, A. Pereira, W. J. Stiekema, *Transgenic Res.* **4**, 288-290 (1995).
49. W. Xuan *et al*., *Curr. Biol.* **25**, 1381-1388 (2015).

50. A. D. Edelstein, M. A. Tsuchida, N. Amodaj, H. Pinkard, R. D. Vale, N. Stuurman, *J. Biol. Methods* **1**, e10 (2014).
51. A. Lampropoulos, Z. Sutikovic, C. Wenzl, I. Maegele, J. U. Lohmann, J. Forner, *PLoS ONE* **8**, e83043 (2013).
52. D. Weijers, J. -P. van Hamburg, E. van Rijn, P. J. J. Hooykaas, R. Offringa, *Plant Physiol*. **133**, 1882-1892 (2003).
53. R. Swarup *et al*., *Nature Cell Biol.* **7**, 1057-1065 (2005).
54. B. Orosa-Puente *et al*., *Science* **362**, 1407-1410 (2018).
55. A. M. Jones, J. Å. H. Danielson, S. N. ManojKumar, V. Lanquar, G. Grossmann, W. B. Frommer, *elife* **3**, e01741 (2014).
56. J. Schindelin *et al*., *Nat. Methods* **9**, 676-682 (2012).
57. R. Haase *et al*., *Nat. Methods.* **17**, 5-6 (2020).
58. J. H. Rowe, A. Rizza, A. M. Jones, in *Environmental Responses in Plants. Methods in Molecular Biology*, P. Duque, D. Szakonyi, Eds. (Humana, New York), vol. 2494, pp. 239-253 (2022).
59. G. Huang *et al*., *Proc. Natl. Acad. Sci. U.S.A.*, **119**, p.e2201072119 (2022).

Acknowledgments

We are highly grateful to Prof. Pedro Luis Rodriguez (CSIC-UPV, Spain) for sharing *pyr/pyl1124589, pyr/pyl1124578* and *pyr/pyl112458* mutants; Prof. Hiroaki Fujii (University of Turku, Finland) for sharing *snrk2.2/3/6*, *snrk2.1/4/5/7/8/9/10* and *snrk2.1/3/4/5/6/7/8/9/10* mutants; Dr. Rui Miao (Fujian Agriculture and Forest University, China) for sharing *hab1-1abi1-2pp2ca, hab1-1abi1-2abi2-2* and *Qabi2-2* mutants. We thank Dr. Lothar Kalmbach, Prof. Yrjö Helariutta (SLCU, UK) and Prof. Niko Geldner (University of Lausanne, Switzerland) for sharing *pSUC2:GFP* seeds. We also thank Prof. Zhizhong Gong and Dr. Wang (China Agricultural University) for kindly sharing *abi1-1* (Col-0) seeds. We acknowledge Prof. Christian Luschnig (University of Natural Resources and Life Sciences – BOKU, Vienna) and Prof. Jiří Friml (IST, Austria) for kindly sharing *eir1-4/PIN2:PIN2-GFP* and *eir1-4/35S:PIN2-GFP* lines. We are grateful to Dr. Frauke Augstein and Dr. Annelie Carlsbecker (Uppsala University, Sweden) for providing *UAS:abi1-1* and driver lines. We thank Dr. François Chaumont (Louvain-la-Neuve, Belgium) and Dr. Anton Schäffner (Helmholtz Zentrum München, Germany) for sharing aquaporin mutant.

Funding

European Molecular Biology Organization Long-Term Fellowship, ALTF 1140-2019 (PM)

European Union's Horizon 2020 research and innovation programme, Marie Skłodowska-Curie, XEROBRANCHING, 891262 (PM)

Biotechnology and Biological Sciences Research Council Discovery Fellowship, BB/V00557X/1 (BKP)

Biotechnology and Biological Sciences Research Council, BB/T001437/1 (MJB, AS)

Biotechnology and Biological Sciences Research Council, BB/V003534/1 (MJB, AS, JB)

Biotechnology and Biological Sciences Research Council, BB/W008874/1 (MJB, CJS)

Biotechnology and Biological Sciences Research Council, BB/W015080/1 (MJB)

Biotechnology and Biological Sciences Research Council, BB/P018572/1 (AMJ)

European Research Council grant, FUTUREROOTS, 294729 (MJB)

European Research Council, SUMOrice, grant agreement No 310235 (AS)

Fonds de la Recherche Scientifique – FNRS (VC)

Swedish Research Council number, 2020-03522 (RPB)

European Research Council, RobustHormoneTrans, 757683 (ES)

NSF Plant Genome Research Program, IOS-1444448 (RES)

Gatsby Charitable Foundation and Biotechnology and Biological Sciences Research Council BB/P018572/1 (AMJ, JR)

European Research Council grant, INTERCELLAR, 725459 (CF)

Biotechnology and Biological Research Council Institute Strategic Programme, Plant Health, BBS/E/J/000PR9796 (CF)

Author contributions

Conceptualization: PM, MJB

Methodology: PM, BKP, VC, JR, HDG

Investigation: PM, BKP, DM, JB, NL, VC, JR, MA, HDG, EM, CJS, RS

Funding acquisition: PM, MJB

Supervision: MJB

Writing – original draft: MJB, PM

Writing – review & editing: PM, BKP, DM, JB, NL, VC, JR, MA, HDG, EM, CJS, RS, SJM, CF, TB, RPB, ES, AMJ, ICD, RES, AS, XD, MJB

Competing interests: Authors declare no competing interests.

Data and materials availability: No restrictions are placed on materials, such as materials transfer agreements. Details of all data are available in the main text or the supplementary materials.

Supplementary Materials

Materials and Methods

Figs. S1 to S33

Tables S1-S2

References (28-59)

Figures

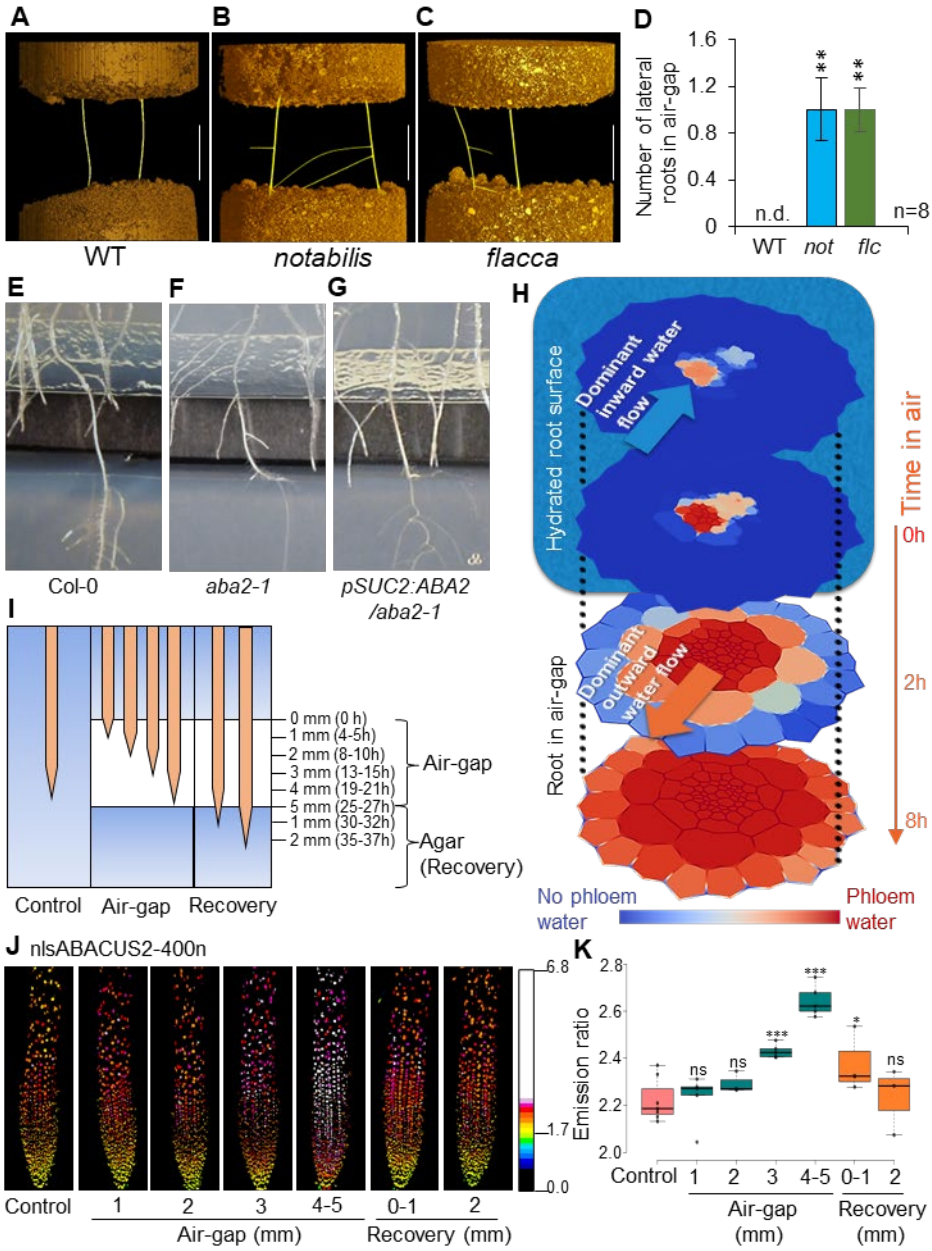

Fig. 1. ABA functions as a repressive signal during xerobranching response. (**A** to **C**) Representative CT images and (**D**) bar-graphs showing xerobranching defect in ABA-deficient tomato mutants (*notabilis*, *flacca*) vs wild-type (WT; Ailsa Craig). Air-gap ~ 1.5 cm. Bar = 1 cm. (**E**) AAA (**A**gar-based **A**ir-gap **A**ssay) system showing xerobranching response in *Arabidopsis* wild-type (Col-0) (air-gap ~5 mm). (**F**) *Arabidopsis* ABA biosynthetic mutant *aba2* produces lateral roots in air-gap. (**G**) Expression of *ABA2* in phloem companion cells rescues xerobranching defect of *aba2*. (**H**) The MECHA hydraulic model predicts phloem as the main source of water in *Arabidopsis* root elongation zone only when located in an air-gap. Simulated water advection maps show dominating phloem water in root epidermal cells within 8 hours. (**I**) For studying temporal response of reporters during xerobranching, primary root tips were grown to different lengths in air-gap (0-5 mm) and recovery (up to 2 mm in moist agar) conditions. (**J**) Emission ratio images and (**K**) box-plots of nlsABACUS2-400n reveal dynamic changes in endogenous ABA levels as root tips grow across air-gap and after recovery. Colour scale represent emission ratios. *, *** and ns represent $P \leq 0.05$, $P \leq 0.001$ and non-significant changes, respectively.

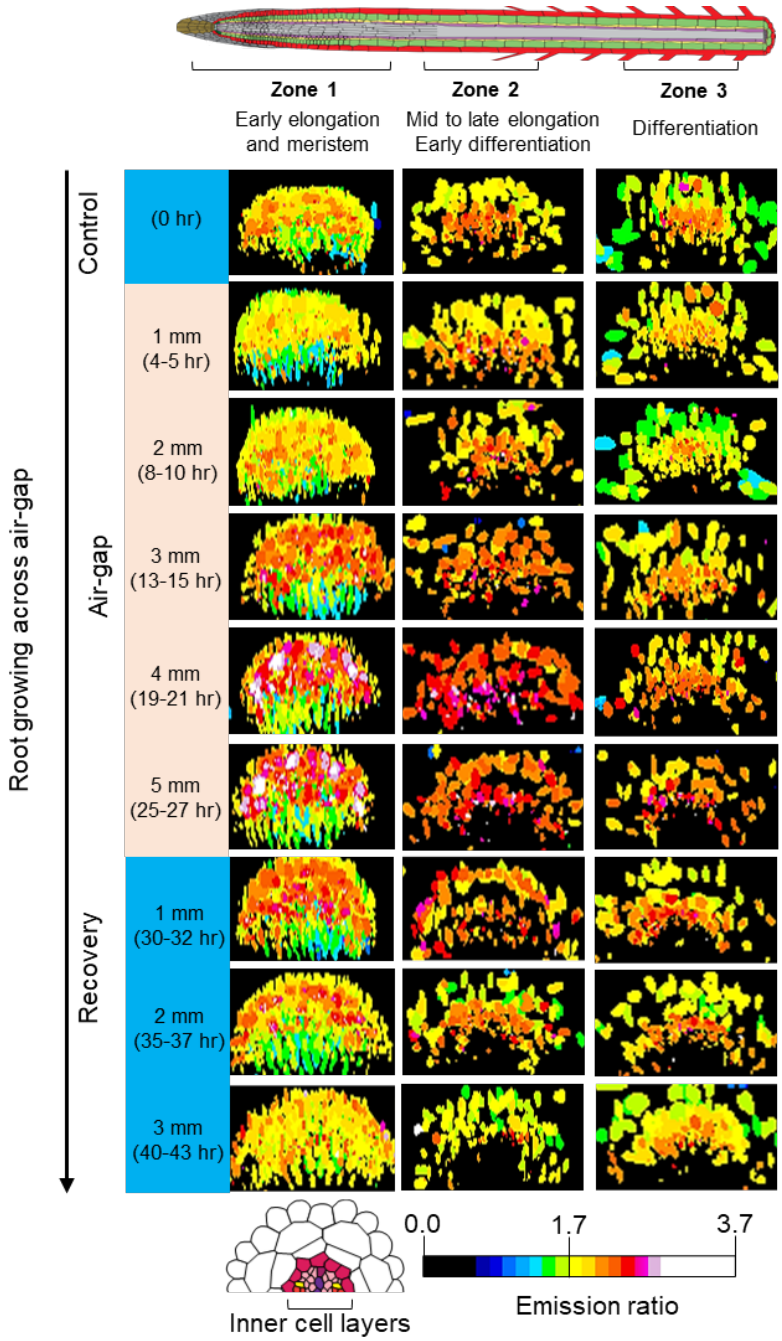

Fig. 2. ABA moves radially outwards following a xerobranching stimulus. Ratio images of *Arabidopsis* roots expressing nlsABACUS2-400n reveal spatiotemporal distribution of ABA as the roots grow across an air-gap. Each image is a representative maximum projection ratio map generated from a stack of several radial cross-sections. Roots were imaged at different time points (indicated by hours) as they exit moist agar (control), grow in a 5mm air-gap and reconnect with agar (recovery). Length (mm) on vertical axis indicates length of root tips in air-gap and recovery conditions. For each time point, cross-sections were generated from different zones of roots marked as zone 1 (early elongation and meristem), zone 2 (mid to late elongation/early differentiation) and zone 3 (differentiation). Radial cross sections from zone 1 (compare cross sections from 1 to 5 mm) reveal an increase in ABA in outer (but not inner) tissues which appears to originate from phloem unloading in zone 2 following a xerobranching stimulus. Colour scale represents FRET emission ratios. Higher ratios correspond to higher ABA concentrations. Experiment was performed with at least four replicates per timepoint per zone ($n=4$).

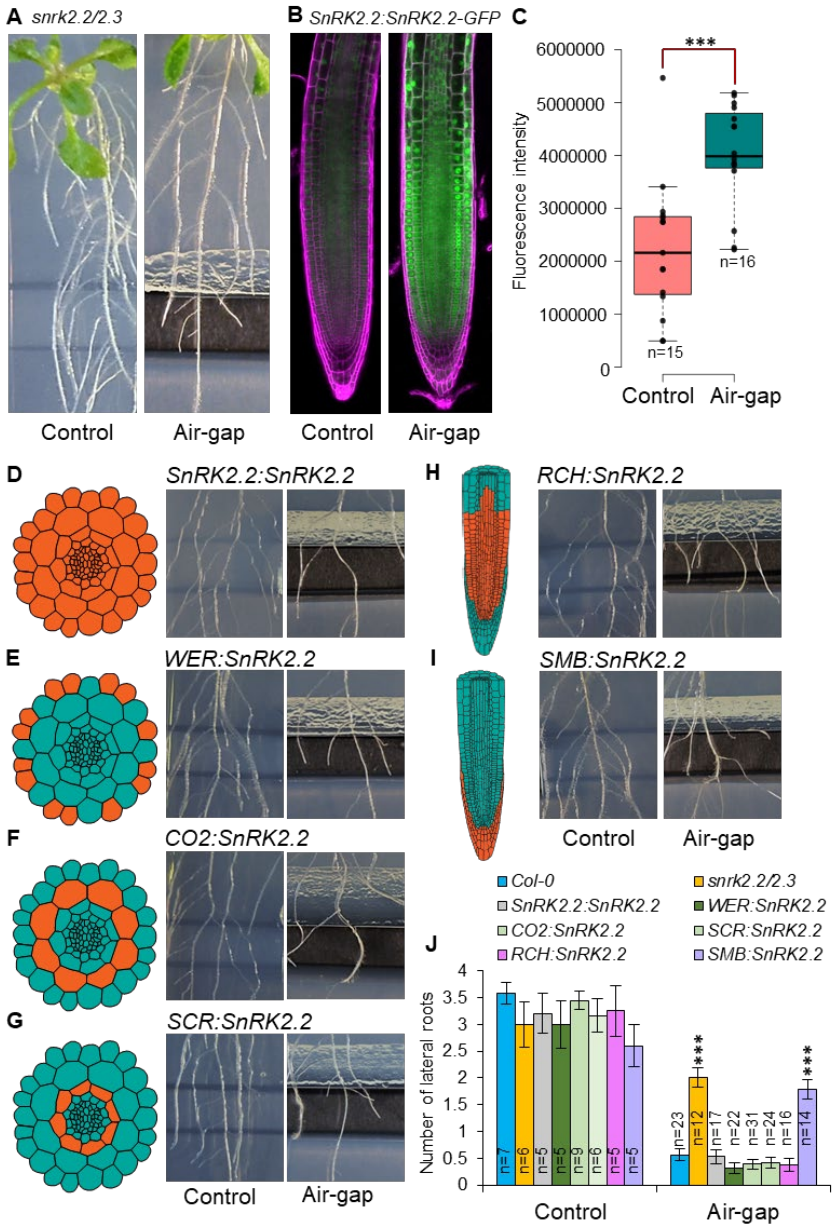

Fig. 3. Xerobranching is dependent on ABA perception in *Arabidopsis* primary root transition zone tissues. (**A**) ABA signalling mutant *snrk2.2/2.3* disrupts xerobranching in AAA system. Air-gap ~ 5 mm. (**B** and **C**) Elevated response of *pSnRK2.2:SnRK2.2-GFP* in root tips subjected to air-gap vs control conditions. Scale bar = 100 µm. (**D**) Expression of *SnRK2.2* under its own promoter rescues the xerobranching defect of *snrk2.2/2.3*. (**E** to **G**) Functional complementation of *snrk2.2/2.3* by tissue specific expression of *SnRK2.2* in epidermis, cortex and endodermis using the *WER*, *CO2* and *SCR* promoters, respectively. (**H**) Root zone specific expression of *SnRK2.2* in root meristem/transition zone (using *RCH* promoter) rescues the xerobranching defect of *snrk2.2/2.3*. (**I**) Expression of *SnRK2.2* in columella and lateral root cap using SMB promoter in *snrk2.2/2.3* background. (**J**) Number of lateral roots produced by wild-type (Col-0), *snrk2.2/2.3* and different tissue/zone specific rescue lines in the air-gap region vs the corresponding region of roots grown under control conditions. Orange colour in root schematics defines the tissue/zone of expression of selected promoters used for complementation. Significant changes with respect to control **(C)** or wild-type **(J)** were calculated by Student's *t*-test. *** represents $P \leq 0.001$.

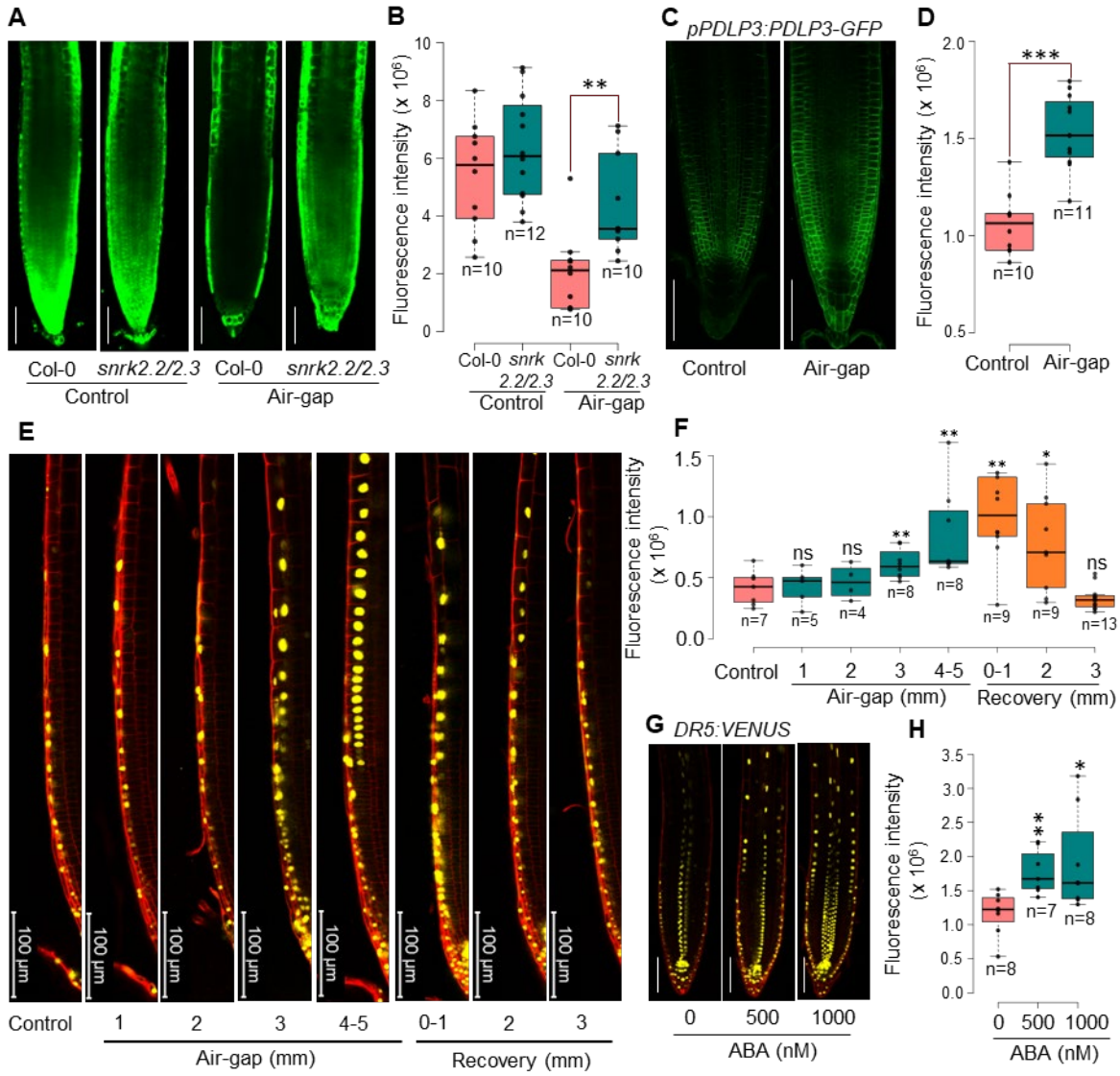

Fig. 4. ABA blocks radial auxin flow by reducing PD permeability causing xerobranching. (**A**) Slower migration of symplastic tracer CF (carboxyfluorescein) in wild-type *Arabidopsis* (Col-0) primary root tips subjected to xerobranching stimulus vs control conditions. CF migration was indistinguishable in ABA signaling mutant *snrk2.2/2.3* with or without the xerobranching stimulus. Root tips were treated with CFDA (carboxyfluorescein diacetate) before imaging. (**B**) CF fluorescence intensity in wild-type and *snrk2.2/2.3* root tips exposed to air-gap vs control conditions. (**C**) Xerobranching stimulus induces expression of *pPDLP3:PDLP3-GFP*. (**D**) Box-plots showing significantly enhanced response of *pPDLP3:PDLP3-GFP* in air-gap vs control conditions. (**E** and **F**) Auxin response reporter *DR5:VENUS* shows higher fluorescence signal in epidermis of root tips exposed to air-gap vs control/recovery conditions. (**G** and **H**) ABA treatments phenocopy *DR5:VENUS* response during xerobranching. Scale bar = 100 µm. *, **, *** and ns represent $P \leq 0.05$, 0.01, 0.001 and non-significant, respectively (Student's *t*-test).

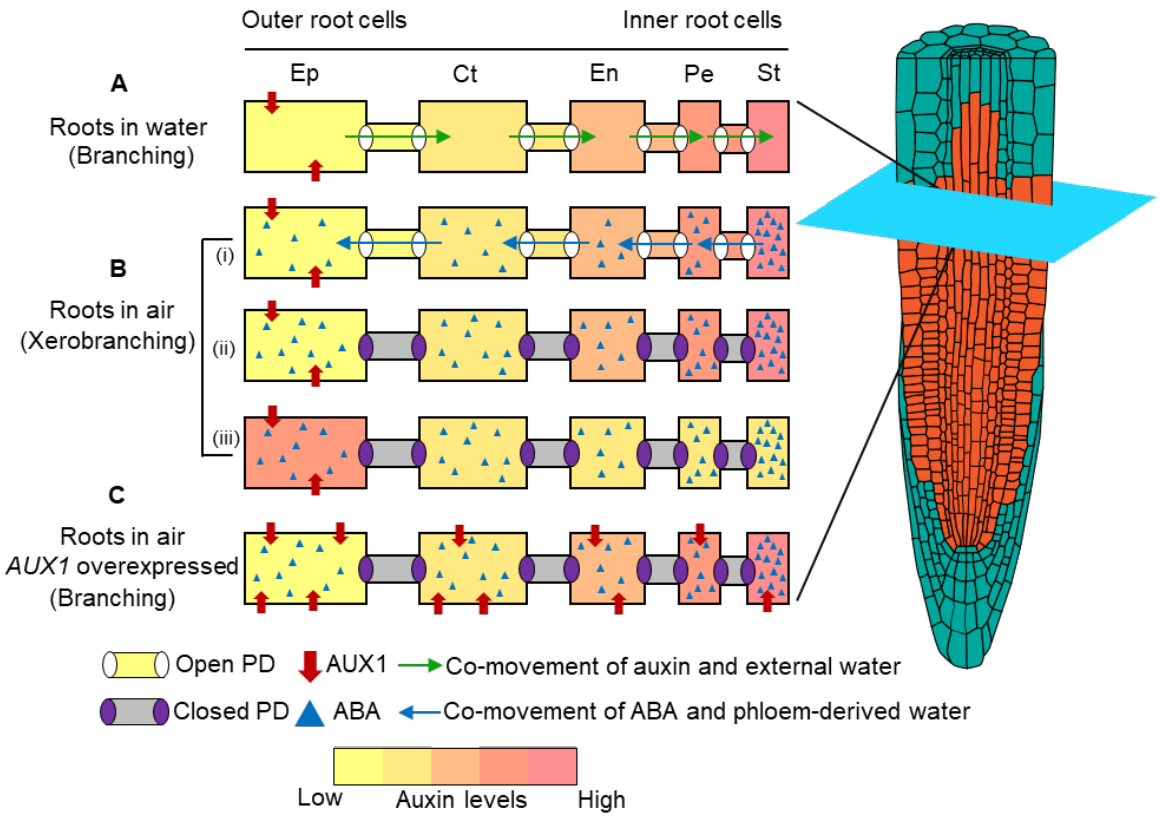

Fig. 5. Dynamic hormone redistribution determines root branching or xerobranching response to external water availability. Schematics illustrate cellular auxin, ABA and water fluxes in root basal meristem (highlighted cell files in transverse root section) exposed to water or air. **(A)** Under normal moisture conditions, roots co-transport water and auxin radially inwards via plasmodesmata (PD) delivering the key hormone signal (auxin) to pericycle (Pe) cells where lateral root initiation is triggered. **(B)** Xerobranching stimulus triggers rise in ABA levels in inner root tissues (St; stele) suppressing root branching. In the transient absence of external water, phloem-derived water co-mobilises ABA from inner (St; stele) to outer root cells (Ep; epidermis) via plasmodesmata (i). ABA induces closure of plasmodesmata through *PDLP*s and *Cals* (ii) disrupting symplastic radial movement of auxin to pericycle (iii). **(C)** Ectopic expression of auxin carriers such as AUX1 in all elongation zone tissue creates a synthetic radial apoplastic auxin pathway which bypasses the disrupted symplastic auxin flow, causing root branching in air-gap. Ep, Ct, En, Pe and St indicate epidermis, cortex, endodermis, pericycle and stele, respectively.